Bioorganic & Medicinal Chemistry 19 (2011) 6645–6653

Contents lists available at ScienceDirect

Bioorganic & Medicinal Chemistry

journal homepage: www.elsevier.com/locate/bmc

Isolation of the β-galactosphingolipid coniferoside using a tumor cell proteome reverse affinity protocol

James J. La Clair [a,*], Abimael D. Rodríguez [b]

[a] Xenobe Research Institute, PO Box 3052, San Diego, CA 92163-1052, United States
[b] Department of Chemistry, University of Puerto Rico, PO Box 23346, UPR Station, San Juan, PR 00931-3346, United States

ARTICLE INFO

Article history:
Available online 24 June 2011

Keywords:
Marine natural products
Proteome
Glycosphingolipids
Affinity purification

ABSTRACT

New approaches are vital to the development of marine natural products (MNP) as therapeutic leads. One of the more time consuming aspects of MNP research arises in the connection between structure and function. Here, we describe an isolation protocol that adapts tumor cell proteomes as a vehicle for MNP isolation therein uniting structural and functional analysis. Application of this method to extracts of the sponge *Agelas conifera* led to the isolation of a unique poly-hydroxybutyrated β-galactosphingolipid, coniferoside.

1. Introduction

A long development period is one of the major obstacles in the translation of marine natural products (MNP) into the clinic.[1] While often rewarding, the long time and associated financial investment has become one reason for the industrial sector to shift towards often more rapid and less expensive synthetic materials.[2] That aside, the unique biological activity locked within natural products continues to provide a vital resource not only for therapeutic development[3] but also as tools for biological research.[4] While marine natural products continue to provide a rich source of biologically active materials, there is an immediate need for methods that expedite the connection between isolation and biological characterization, and thereby reduce the time, and hence costs, associated with marine natural products discovery.

Figure 1 provides an overview of the current MNP discovery pathway. The process begins by specimen collection, which traditionally has focused on sampling macroorganisms such as sponges, corals and algae. More recently, the field has moved towards sampling microbial diversity and identifying their metabolites through strain optimization and culturing. While effective, both of these processes result in extracts that are processed through similar chromatographic methods. A number of excellent reviews provide an overview of the recent advances in accessing microbial diversity.[5–7]

The next step in the process, noted by a star in Figure 1, is the most critical to the discovery process and often the longest. Here, a series of chromatographic methods are applied, usually accompanied by bioassay or spectroscopic guidance, to obtain a pure natural product. Recently, this process has been advanced by applying library techniques to fractionate single or multiple compound fractions.[9–11] Using these materials, a combination of spectroscopic methods are then applied to identify the structure of the isolated compound. Often the structure elucidation process begins at a stage in which the isolated compounds' biological activity has yet to be examined. This can lead to the isolation of inactive leads.

In 2008, we described a bidirectional affinity procedure to simultaneously isolate natural products and identify their biomolecular targets using a combination of forward and reverse techniques.[12] Using this approach, we were able to determine that the marine natural product, sceptrin (structure provided in Fig. 1), bound to the bacterial equivalent of actin, MreB. Here, we describe a system to screen for compounds displaying potent activity against tumor cell progression using the proteins from within the target cell as the vehicle for purification.

2. Results and discussion

Our studies began by developing a reverse affinity resin system using protein lysates from the HCT-116 human colorectal carcinoma cell line. HCT-116 cells were cultured using a Fiber Cell device, collected and lysed. Concerned that the whole cell proteome would not deliver sufficient selectivity, we subcellularly fractioned the cells (see Section 4). A total of five fractions were prepared according to procedures to isolate the: cytosol (**R1**), mitochondria, perioxosomes, and lysosomes (**R2**), Golgi apparatus (**R3**), nucleus (**R4**) and endoplasmic reticulum and plasma membrane (**R5**). Samples of each fraction were treated with protease inhibitors,

* Corresponding author.
E-mail addresses: i@xenobe.org (J.J. La Clair), abrodriguez@uprrp.edu (A.D. Rodríguez).

0968-0896/$ - see front matter © 2011 Published by Elsevier Ltd.
doi:10.1016/j.bmc.2011.06.051

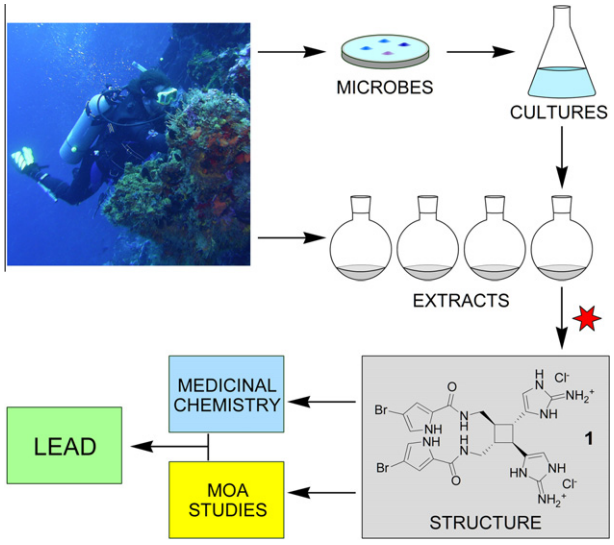

Figure 1. The current pathway used in marine natural products discovery. The process begins by field exploration and specimen collection. Extracts are then prepared from these specimens either through strain selection and culturing or conventional extraction. The next and key step, noted by a star, examines the isolation of pure compounds and their structure elucidation. Once a molecular structure is attained, samples of the natural product are then advanced into leads by a combination of medicinal chemical, and chemical biological studies. Ideally, these include determination of the mode of action (MOA) of the natural product.[8]

lysed (as needed), and concentrated to 5 mg/mL in total protein (see Fig. 2).

Samples of each fractionated lysate were incubated with Affi-Gel 10 resin to deliver five different resins **R1**–**R5** containing tumor cell proteins from a different subcellular fraction (see Section 4). Using multiple batches, 30–50 mL of resin were prepared from each of the five subcellular fractions **R1**–**R5**. A combination of A_{280} measurements and a quantification kit (Bio-Rad Protein Assay) were used to determine the protein concentration on each resin as given by 3.2 ± 0.7 mg/mL for **R1**, 2.1 ± 0.3 mg/mL for **R2**, 1.2 ± 0.3 mg/mL for **R3**, 3.2 ± 0.3 mg/mL for **R4**, and 2.2 ± 0.4 mg/mL for **R5**.

A 25 mL aliquot of each resin was loaded into a cartridge. The cartridges were then assembled in series along with a pump and tank as depicted in Figure 3. The tank was then charged with 854 mg of *Agelas conifera* extract **E1** dissolved in 1 L of PBS pH 7.2 containing 0.5% DMSO. The extract was pumped for 12 h at 4 °C through the resin cartridges. After this period, the extract solution was removed from the tank and the system was purged by sequential washes with PBS pH 7.2 and deionized water.

The resin cartridges were then removed from the system and bound natural products were then eluted by passage of warm 95% EtOH (see Section 4). The resulting materials were dried via rotary evaporation to deliver 28.2 mg from **R1**, 3.2 mg from **R2**, 1.2 mg from **R3**, 1.8 mg from **R4**, and 32.1 mg from **R5**.

We then examined each fraction by LC/MS (see Fig. 4). Only traces of compounds were observed in the fractions obtained from resins **R2**–**R4**, and therefore they were not evaluated further. Fractions from columns with resins **R1** and **R5**, however, contained a consistent series of five peaks corresponding to compounds **1**–**5**. While the separation was effective, MS analyses conducted during HPLC separation on collected fractions using either electron impact (EI) or electrospray ionization (ESI) failed to provide a consistent ionization and therefore the *m/z* of each peak could not be determined. We were, however, able to dissolve each material in $CDCl_3$ and collect NMR data on each fraction (^{1}H NMR spectra are provided in Fig. 5).

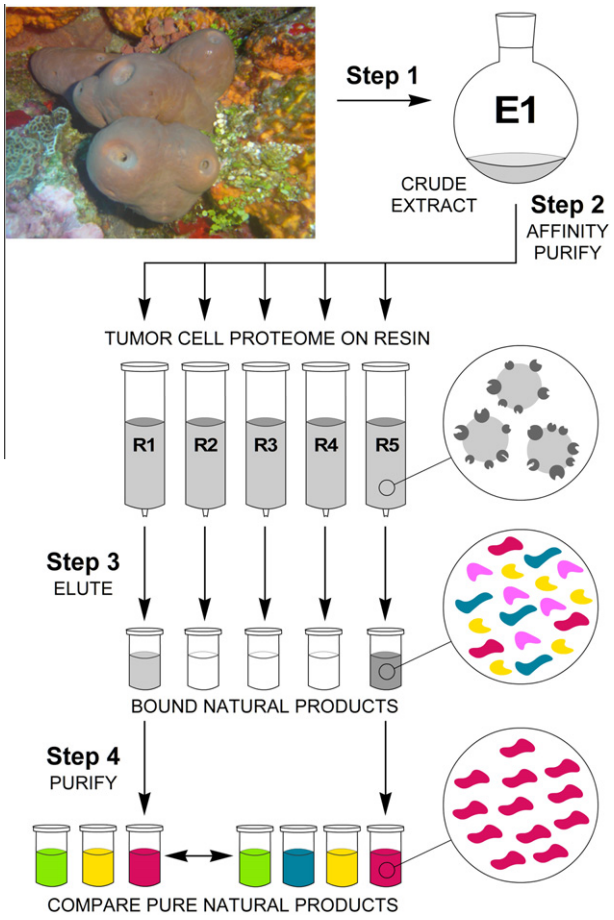

Figure 2. Protocol for reverse affinity isolation of compounds that bind to proteins in the HCT-116 tumor cell proteome. (Step 1) Crude extracts from *A. conifera* specimens, **E1**, were prepared, dried, and dissolved in 1 L of PBS pH 7.2 containing 0.5% DMSO. (Step 2) Each extract solution was circulated through a series of five subcellularly fractionated proteomic resin columns **R1**–**R5** for 12 h at 4 °C, then washed with PBS pH 7.2 and H_2O. (Step 3) Each column was removed from the system, and the bound materials were eluted with warm 95% EtOH.

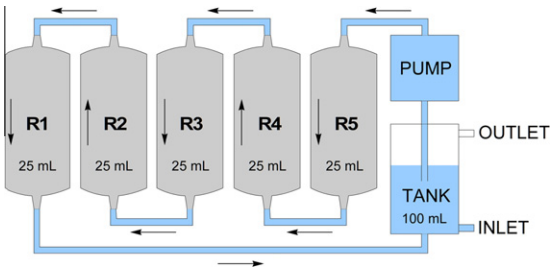

Figure 3. Schematic representation of the reverse affinity extractor. The system contains five affinity columns **R1**–**R5** that are attached in series with Tygon tubing to a microliquid OEM pump and a tank. The natural products extracts were added to the tank via the inlet (see Section 4).

We then turned to HPTLC to obtain pure compounds. An aliquot of **R1** (25.2 mg) was applied to a C18 HPTLC plate (EM Sciences) to obtain 1.2 mg of **1**, 1.6 mg of **2**, 0.9 mg of **3**, 5.2 mg of **4** and 3.2 mg of **5**. Application of this method to 24.2 mg of fraction **R5** provided an additional 2.1 mg of **1**, 2.4 mg of **2**, 1.6 mg of **3**, 3.1 mg of **4** and 4.2 mg of **5**. The purity of each compound was determined to be above 95% by HPLC analysis. We confirmed that each compound in **R1** and **R5** was assigned as shown in Figure 4 by spiking samples of the latter fraction with pure compounds **1**–**5**.

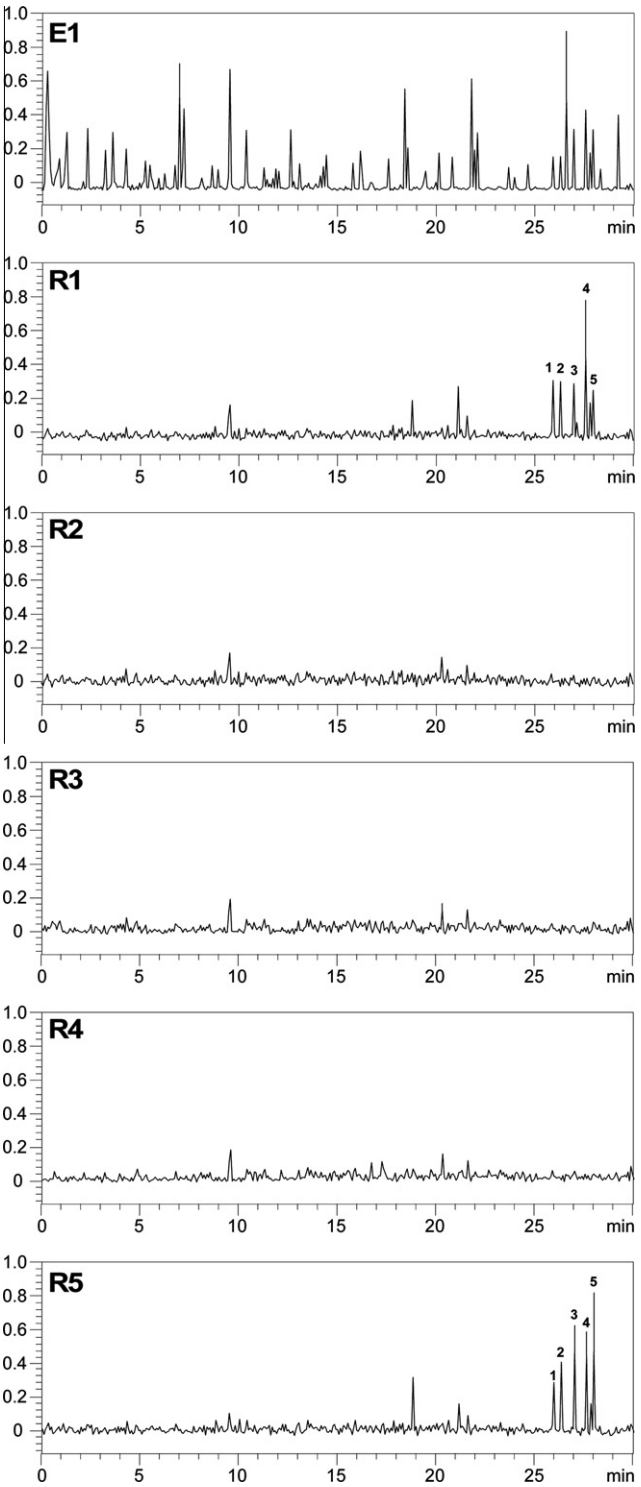

Figure 4. Traces from LC/MS analysis of the crude extract **E1** and fractions eluted from resins **R1**–**R5**.

Our efforts then focused on elucidating the structure of the major component compound **4**. A dataset containing ^{1}H, ^{13}C, ^{13}C-DEPT, gCOSY, TOCSY, NOESY, HSQC and HMBC spectra was collected in a 3:1 mixture of $CDCl_3$:CD_3OD. Comparison of the ^{1}H NMR data from **4** (Fig. 6) with those of the crude fraction **R1** (Fig. 5) suggested that **4** was the major component in this fraction. This was also supported by HPLC analysis and the amount of material obtained after HPTLC purification.

Analysis of the NMR dataset (Table 1) suggested that compound **4** contained four structural fragments as given by a carbohydrate, sphinganine, fatty acid, and hydroxyester. We began by evaluating the carbohydrate fragment using gCOSY, TOCSY and ROESY data. First we identified the anomeric proton H-1′ at δ 4.20 by its correlations with H-2′ in the gCOSY spectrum and long-range couplings to H-3′ in the TOCSY spectrum. The coupling between H-1′ and H-2′, $^{3}J_{HH}$ = 7.8 Hz, indicated that the anomeric center was β-oriented. This was further supported by the rather downfield chemical shift of C-1′ at δ 103.0 as well as strong NOEs between H-1′ and H-3′ and between H-1′ and H-5′. Using these data along with additional gCOSY, TOCSY and ROESY correlations (Fig. 7), we were able to assign the remaining protons on the carbohydrate motif (Table 1). The observation of NOEs between H-1′ and H-3′, between H-1′ and H-5′, and between H-4′ and the protons at H-6′ suggested that the carbohydrate was a galactoside, a well recognized unit in sponge-derived sphingolipids.[13–15] We then turned to the HSQC, ^{13}C-DEPT and HMBC spectra to assign the corresponding carbon atoms. Complete assignments for the proton and carbon atoms within the carbohydrate unit are noted in Table 1.

The anomeric proton H-1′ also provided a direct link to the sphinganine fragment as given by correlations from H-1′ to H-1, H-2, and H-3 in the ROESY spectrum (Fig. 7). The gCOSY spectrum identified two fragments with correlations between each proton from H-1 to H-14 and H16 to H19. These conclusions were also supported by long-range couplings observed in the TOCSY spectrum and NOE correlations in the ROESY spectrum. In particular, correlations from H-2 to H-4, H-4 to H-7 and H-7 to H-9 in the ROESY spectrum (Fig. 7) provided strong support for these assignments. These data were then used to assign each carbon atom using the combination of HSQC, ^{13}C-DEPT and HMBC data as given in Table 1. While effective, these datasets failed to provide a definitive assignment of the proton and carbon atoms at C-14, C-15, C-16 and C-17, due in part to their overlapping signals.

We then turned to the fatty acid fragment. Analysis of the HMBC spectrum provided a direct correlation between the proton on C-2 and the carbonyl at C-1″. A second correlation was also observed from the proton on C-2″ to the C-1″ carbonyl. Using these observations along with the correlations observed in the gCOSY, TOCSY and ROESY spectra (key interactions are shown in Fig. 7), we were able to identify a direct linkage between C-1″ and C-5″, however, once again the redundancy within the adjacent lipid chain prevented further assignment.

At this stage, three structural motifs within the fatty acid and hydroxyester subunits remained unassigned. The first motif was a *trans*-di-substituted olefin, ascribed as H-14″–H-15″, whose correlations within the gCOSY, TOCSY and ROESY spectra suggested that it was positioned within the fatty side chain. Due to the overlap of the aliphatic groups, unambiguous assignment of its position was not possible. While depicted as *trans*-, the C-14″–C-15″ could also be a *cis*-olefin.

The second motif contained three sets of peaks. The first was a methylene group adjacent to a carbonyl with δ_H 2.24 (H-5‴ and H-9‴) and δ_C 34.0 (C-5‴ and C-9‴) that showed a clear correlation to a carbonyl at δ_C 175.6 (C-4‴ and C-8‴) in the HMBC spectrum. The second also consisted of a methylene group bearing an acyloxy moiety with δ_H 3.93 (H-7‴). It also coupled to the carbonyl at δ_C 175.6 in the HMBC spectrum. The third set of peaks was an aliphatic methylene unit (H-6‴ and H-10‴) that was mutually coupled to the prior two peaks as indicated by correlations in the gCOSY spectrum. Analysis of the HSQC and ^{13}C-DEPT spectra indicated that each peak in the proton spectrum correlated with up to five methylene (CH_2) carbons. Analysis of the integration in the ^{1}H NMR spectrum suggested that this unit was a pentamer. On further analysis, the chemical shift of the protons on one of the methylene

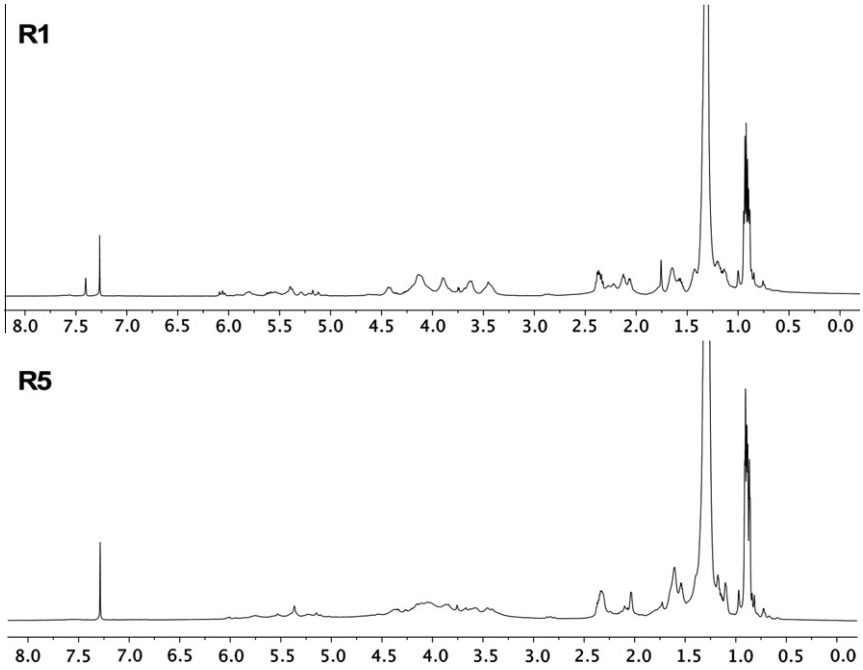

Figure 5. ^{1}H NMR spectra collected at 500 MHz on samples of fractions **R1** and **R5** dissolved in $CDCl_3$ containing 5% CD_3OD.

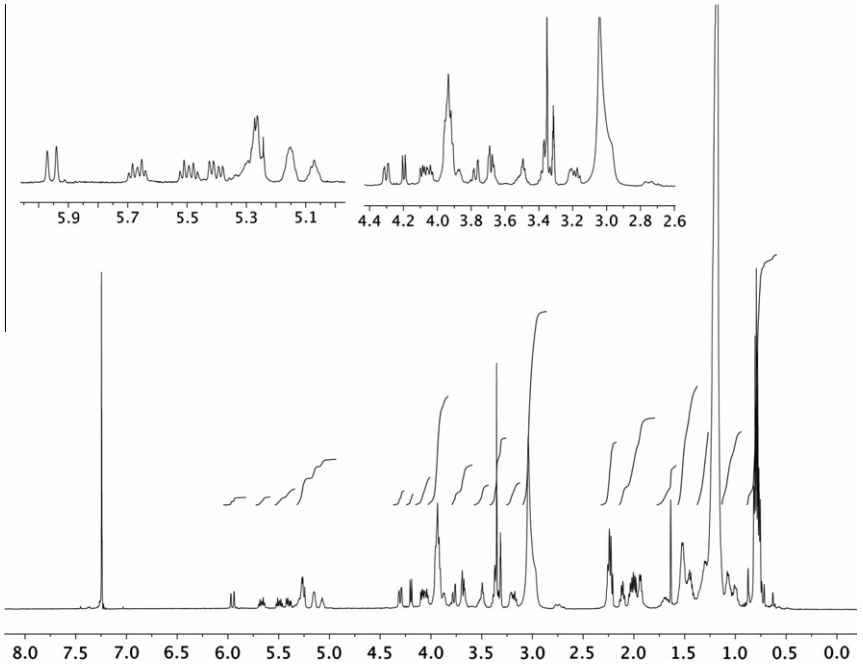

Figure 6. A 500 MHz ^{1}H NMR spectrum of compound **4** in 3:1 $CDCl_3/CD_3OD$. Insets provide expansion of the peaks observed between δ 5.00–6.00 and δ 2.60–4.40, respectively.

units appeared at δ_H 3.35 (H-11‴) and δ_C 50.1 (C-11‴) suggesting that this was a terminal unit.

The third and final motif was comprised of three protons that existed in an ABX pattern. The first proton at δ_H 5.15 (H-2‴) coupled with a $^{3}J_{HH}$ = 2.1 and 6.9 Hz to protons at δ_H 4.30 (H-3a‴) and 4.08 (H-3b‴), respectively. The proton at δ_H 4.30 was geminally-coupled to the proton at δ_H 4.08 with a $^{2}J_{HH}$ ~12.0 Hz. These data suggested the presence in 4 of a glycerate subunit C–1‴ to C–3‴.

Next, to support the molecular structure of **4**, we returned to MS analysis to identify the remaining carbon motif. While multiple attempts were made using MALDI, FAB, ESI, and EI methods in both negative and positive ion modes, we failed to detect a distinctive parent ion. In all the methods examined, we observed sets of peaks that appeared to have a consistent fragmentation with loss of 86 amus. While exhaustive attempts were conducted, it was becoming clear to us that this sample contained a mixture of homologs with differing fatty acid chain lengths, a common feature of galactosphingolipids.[13–15] Thus, we turned to degradation methods to confirm this observation.

Using procedures developed by Fattorusso and Mangoni,[13] we applied degradative methods to the analysis of 120 μg sample of

Table 1
^{1}H and ^{13}C NMR data on coniferoside (**4**) in 3:1 $CDCl_3/CD_3OD$

Position	δ_H (mult, *J* in Hz)	δ_C (mult)[a]
1	3.68 (m)	68.5 (CH_2)
2	3.87 (m)	68.6 (CH)
3	3.52 (m)	71.7 (CH)
4	4.04 (m)	72.1 (CH)
5	5.40 (dd, 6.9, 15.5)	129.1 (CH)
6	5.67 (td, 6.5, 15.0)	133.8 (CH)
7a	2.04 (d, 6.6)	32.7 (CH_2)
7b	2.01 (d, 7.0)	
8a	2.13 (d, 7.8)	27.7 (CH_2)
8b	2.10 (d, 7.4)	
9	5.28 (m)	129.3 (CH)
10		129.1 (C)
11	5.96 (d, 15.6)	134.4 (CH)
12	5.49 (td, 7.0, 15.5)	128.8 (CH)
13	2.00 (dd, 6.6, 13.9)	32.7 (CH_2)
14–17	1.18 (m)[c]	19.3, 22.5, 22.6, 29.5 (CH_2)[c]
18	0.99 (m)[c]	36.8 (CH_2)[c]
19	0.78 (m)[c]	13.7 (CH_3)[c]
20	1.64 (s)	12.6 (CH_3)
1′	4.20 (d, 7.8)	103.0 (CH)
2′	3.18 (dd, 7.8, 8.9)	73.2 (CH)
3′	3.36 (m)	76.1 (CH)[b]
4′	3.36 (m)	69.2 (CH)[b]
5′	3.21 (m)	75.9 (CH)
6a′	3.68 (m)	61.3 (CH_2)
6b′	3.77 (dd, 2.3, 12.2)	
1″		174.5 (C)
2″	5.07 (m)	71.5 (CH)
3″	3.51 (m)	68.9 (CH)
4″	3.93 (m)	72.2 (CH)[b]
5″	1.72 (m)	34.4 (CH_2)
6″–12″	1.18 (m)	24.8, 25.2 (CH_2)[b,c]
13a″	1.95 (d, 5.7)	27.0 (CH_2)
13b″	1.93 (d, 5.6)	
14″	5.26 (m)	129.5 (CH)
15″	5.26 (m)	129.5 (CH)
16a″	1.95 (d, 5.8)	27.0 (CH_2)
16b″	1.93 (d, 5.5)	
17″–22″	1.18 (m)[c]	22.7, 29.5, 32.1, 36.9 (CH_2)[b,c] (CH_2)[b]
23″	1.07 (m)[c]	39.0 (CH_2)[b,c]
24″	0.78 (m)[c]	11.1 (CH_3)[b,c]
1‴		175.7 (C) [b]
2‴	5.15 (m)	70.1 (CH)
3a‴	4.30 (dd, 2.1, 11.7)	62.3 (CH_2)
3b‴	4.08 (dd, 6.9, 12.8)	
4‴,8‴		175.6 (C)[b]
5‴,9‴	2.24 (m)	34.0 (CH_2)[c]
6‴,10‴	1.45 (m), 1.52 (m)	22.2, 29.5, 32.2 (CH_2)[b,c]
7‴	3.93 (m)	64.2, 66.1, 72.2 (CH_2)[b,c]
11‴	3.35 (m)	50.1 (CH_2)

[a] ^{13}C Assignments were made by evaluation of the ^{13}C, ^{13}C-DEPT, HSQC, and HMBC spectra.
[b] These assignments were made based on comparing the gCOSY, TOCSY and NOESY data with correlations in the HSQC spectrum. However, the widespread coalescence of multiple peaks made definitive assignments difficult.
[c] This position was observed as an isomeric mixture and each proton or carbon observed was reported.

4. We were able to confirm the presence of the galactoside by identifying α-methyl-2,3,4,6-tetra-*O*-benzoyl-D-galactose from the aqueous hydrolytic fraction (fraction **A**, Fig. 8). However, the digestion procedure required scale-up in order to provide a clear interpretation of the remaining fragments.

By running the process on 1 mg of **4**, we were able to obtain sufficient organic soluble fraction **B** (Fig. 8), which upon benzoylation and purification provided ~0.2 mg of a benzoylated sphinganine (fraction **D**, Fig. 8). High-resolution ESIMS analysis indicated that this material was correctly assigned by the observation of an exact mass for $M+Na^+$ at *m/z* 778.3724 (calcd for $C_{48}H_{53}NNaO_7$, *m/z* 778.3720) along with a minor $M+Na^+$ at *m/z* 764.3559 (calcd for $C_{47}H_{51}NNaO_7$, *m/z* 764.3563). The fact that the observed mass in fraction **D** was *m/z* 778.3724 supported the presence of nitrogen at C-2 in **4**, as the corresponding ester would be one atomic mass unit higher (calcd for $C_{48}H_{52}NaO_8$, *m/z* 779.3560). In addition, we collected gCOSY and TOCSY spectra on **4** in $CDCl_3$ containing 10% pyridine for solubilization. In both spectra, we observed an NH proton at δ_H 7.48 that coupled to H-2 in the gCOSY spectrum and H-1, H-2 and H-3 in the TOCSY spectrum. These two pieces of evidence provided convincing support for the presence of an amide at C-2.

We turned to an oxidative sequence to evaluate the lipid terminus of the sphinganine fragment. Lemieux oxidation of a sample of fraction **D** with a mixture of $KMnO_4$ and $NaIO_4$ followed by esterification with trimethylsilyldiazomethane identified the terminus of the sphinganine fragment as either a 7- or 8-carbon chain linear or an 8-carbon branched chain, as shown in **E** (Fig. 8).

By applying the Lemieux oxidation to the $CHCl_3$ fraction **B** (Fig. 8) and evaluating by GC/MS analysis, we were able to further confirm the terminus of the sphinganine fragment as well as determine that the fatty acid terminus contained a 10- to 12-carbon chain (see **C** in Fig. 8). In addition, we obtained two peaks in the GC whose MS analysis provided ions that corresponded to glyceric acid ($M+H^+$ *m/z* of 107.04) and methyl 2,3-dihydroxypropanoate ($M+H^+$ *m/z* of 121.06), both peaks were confirmed by spiking with authentic standards. Returning to the NMR dataset, we determined that a glycerate unit fit the assignments for the proton and carbons from C-1‴ to C-3‴. The HMBC spectrum indicated that C-1‴ was adjacent to C-4″ on the fatty acid fragment as shown in Figure 7. Analysis of the HMBC spectrum also indicated that the oligomeric hydroxyester fragment was then attached at C-3‴.

At this point, the only remaining fragment to be elucidated was the oligomeric hydroxyester. By reducing the temperature of the hydrolytic conditions from 80 °C to 23 °C (**F**, Fig. 8), we were able to observe a peak with M^+ at *m/z* 86.2 by GC/MS analysis that when compared to an authentic standard matched the retention time of γ-butyrolactone. This observation was in agreement with the NMR data and confirmed the presence of a poly-4-hydroxybutyrate (P4HB) unit.

This observation was also consistent with the NMR data. Analysis of the HMBC spectra provided a direct correlation between H-3‴ and the carbonyl at C-4‴ indicating that the P4HB unit was attached via the C-3‴ carbinol of the glycerate. Further analysis also confirmed the assignment of the terminal carbon of this fragment, C-11‴, which appeared at a distinct position as given by δ_H 3.35 (H-11‴) and δ_C 50.1 (C-11‴). Additionally, the presence of the P4HB unit (arguably the reason for the rapid fragmentation during MS analysis on **4**) along with the diversity of fatty acid chain lengths explain our inability to identify the parent ion of **4**.

A combination of NMR and degradation studies provided strong support for the structure of **4**. However, questions remain regarding the stereochemical assignments, and without synthetic standards of each fragment, this effort could not be completed. Furthermore, the methods used herein failed to provide a definitive assignment for the position and stereochemistry of the olefins at C9–C10 and at C-14″–C-15″. The answers to these questions as well as a detailed structural confirmation of **4** can be determined through the total synthesis or by the synthesis of the fragments obtained during our degradation studies (Fig. 8). These objectives, however, remain outside the scope of this investigation.

3. Conclusion

The use of protein affinity resins offers great potential for natural products isolation. In this study, we demonstrate the use of a

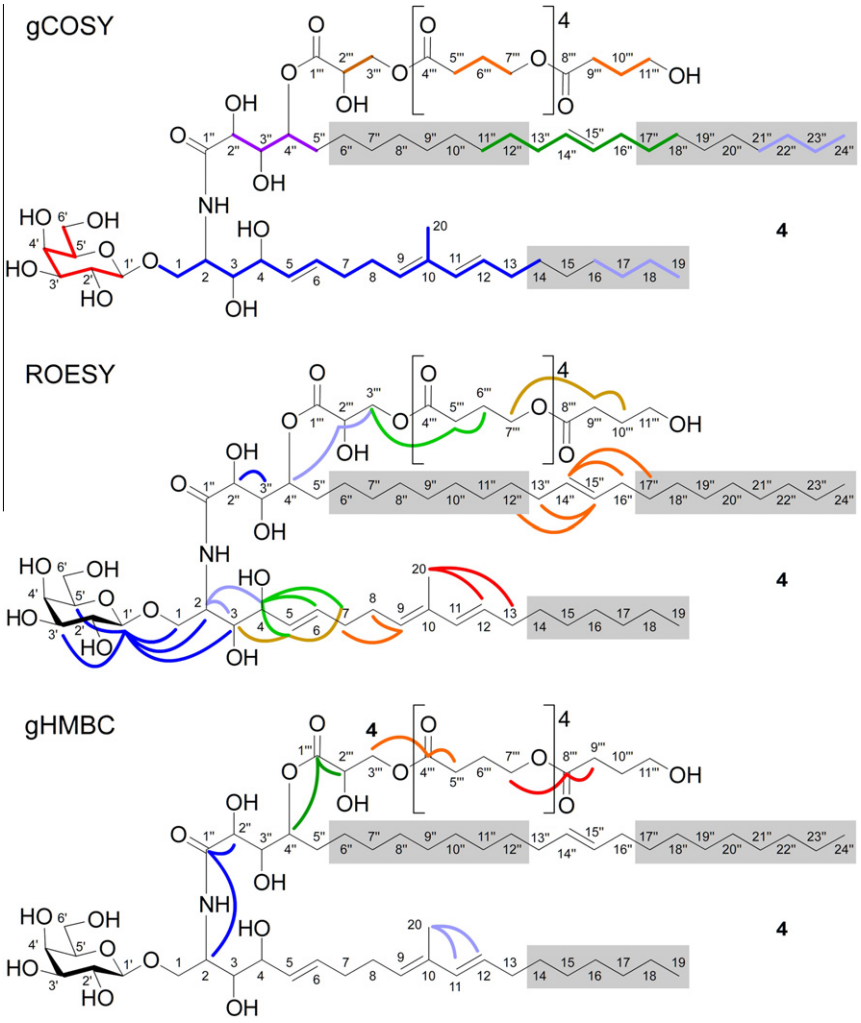

Figure 7. Structure of coniferoside (**4**) including key gCOSY, ROESY and gHMBC correlations. Variable regions are shaded in grey.

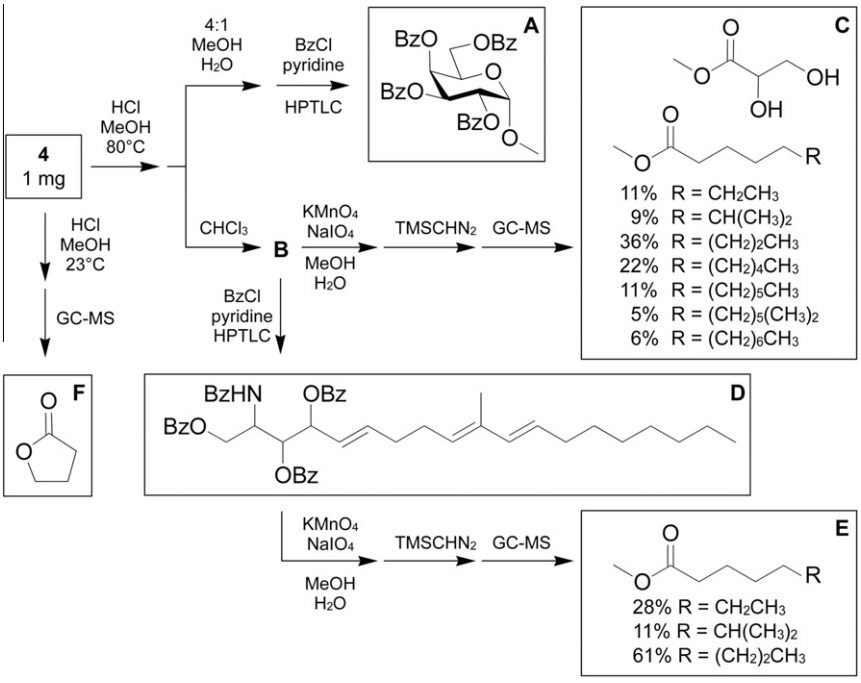

Figure 8. Degradation studies on coniferoside (**4**) support the structures of the carbohydrate, sphinganine, fatty acid and hydroxyester fragments. Percentages note the abundance of each isomer observed.

subcellularly-fractionated proteome from tumor cells to guide the isolation of a complex poly-hydroxybutyrated β-galactosphingolipid, coniferoside (**4**). Compound **4** was observed in the cytosolic and plasma membrane fractions, subcellular regions that are rich in sphingolipids.[16,17] This fact suggests that the protein affinity method provided an active role in the isolation of **4**. NMR analysis on the crude fractions R1 and R5 also suggest that the other compounds **1**, **2**, **3** and **5** are likely related sphingolipids (see Fig. 5).

In conclusion, this study demonstrates the use of protein-guided methods to isolate a compound by its affinity to proteins within tumor cell proteomes. Analysis of the activity of **4** in HCT-116 cells, IC_{50} value of 12.2 ± 0.3 nM using the MTT assay[18] with etoposide, IC_{50} value of 3.2 ± 0.5 μM, as a positive control, confirms that this approach is capable of identifying compounds that not only target proteins within an ascribed tumor cell line but also deliver potent cell inhibitor activity. We also note that comparable activity has been observed in natural and synthetic galactosylsphingolipids.[19–21]

This application of affinity resins resulted in the isolation and characterization of a β-galactosphingolipid containing a unique poly-4-hydroxylbutyrate. The fact that mild methods were used for the isolation of **4** suggests that comparable hydroxybutyration may exist elsewhere and may not be detected due to degradation during chromatographic purification or fragmentation during MS analysis. It also supports the high molecular complexity observed in *Agelas* sponges.[22] Finally, we note that hydroxybutyrates are a homopolymer commonly associated with bacteria and have been shown to have a symbiotic role in legumes.[23] Its presence on a sponge-derived galactosphingolipid may suggest a direct symbiotic relationship between sponges and their bacterial symbionts, wherein poly-hydroxybutyrates produced by bacterial guests are stored within the sponge's glycosphingolipids.

4. Methods

4.1. General methods

Optical rotations were determined on a Perkin–Elmer-241 MC polarimeter. UV–vis spectra were collected on a PTI QuantaMaster UV–vis steady state spectrofluorometer with a 0.1 cm quartz cell at 23 °C. FT-IR spectra were collected using a thin film on a NaCl plate using a Perkin Elmer Spectrum One FT-IR spectrometer. HRMS spectra were collected on a ThermoFinnigan MAT900XL-MS. NMR data were recorded on a Bruker DMX500. Samples were dissolved in a mixture of $CDCl_3$ and CD_3OD in 5 mm NMR tubes (Norell Inc.). Chemical shifts were reported relative to the $CDCl_3$ solvent peak (δ_H at 7.24 and δ_C at 77.23). Parameters for the HMBC spectra were optimized for J_{CH} = 8 Hz. NMR spectra were processed with MestreNova Version 6.0.2 (Mestrelab Research S. L.). Solvents were purchased from VWR Scientific or Fisher Scientific and were used as is. Unless otherwise indicated, solvent ratios are noted in (v:v). HPLC, LC/MS and GC/MS analyses were conducted from multiple instruments, columns and solvent mixtures. Exemplary conditions include the use of a Waters model 600E liquid chromatograph with a Waters Wisp 712 autoinjector and a Waters 486 tunable absorbance detector. HPLC analysis was conducted on a 4.5 × 250 mm Beckman Ultrasphere C18 (5 μm) ion pairing or Waters Symmetry C8 (5 μm) column at 23 °C. Exemplary conditions include isocratic runs with 20% aq MeOH (5:1 MeOH/H_2O), 30% aq MeOH, 45% aq MeOH, as well as 35 min binary linear gradient from H_2O to 5% aq MeOH. Detection was conducted with diode array detection monitored at 254 nm. The mass to charge ratios of the identified peaks were determined by collection of the eluted fractions followed by MS analysis or by direct LC/MS analysis. GC/MS analyses were collected on a Thermo Traceplus GC/MS with EI source and single quadrupole MS analyzer using an RTX-5MS column (15 m length and 0.25 mm ID) with a split mode injector.

4.2. Subcellular fractionation

Two methods were used to prepare the subcellularly fractionated protein lysates. Ultracentrifugation was used to prepare HCT-116 cell fractions containing: the cytosol for resin **R1**, the mitochondria, lysosomes, and peroxisomes for resin **R2,** nuclei for resin **R4**, and the endoplasmic reticulum and plasma membranes for resin **R5**. The Golgi apparatus fraction for resin **R3** was prepared separately. General procedure: a frozen and thawed pellet of HCT-116 cells was suspended at 0.25 g/mL of cells in lysis buffer containing phosphate-buffered saline (PBS) pH 7.2, 1% Triton X100, and 0.1% SDS. The cells were ruptured by repeated passage through a 28-gauge needle. A nuclei pellet was collected after centrifugation at 800 rpm for 10 min. A pellet containing mitochondria, lysosomes, and peroxisomes was collected after centrifugation of the remaining supernate at 15,000 rpm for 10 min. The endoplasmic reticulum and plasma membrane were pelleted after centrifugation of the remaining supernate at 100,000 rpm for 60 min. Each pellet was diluted with lysis buffer containing PBS pH 7.2, 1% Triton X100, 0.1% SDS, and a protease inhibitor cocktail (Sigma–Aldrich), ruptured by ultrasonification, and concentrated to 5 mg/mL in net protein by spin dialysis on a 9 kDa MWCO iCON spin concentrator (Pierce). The cytosol fraction was obtained after collecting the supernate after centrifugation at 200,000 rpm for 3 h followed by concentration to 5.0 ± 0.2 mg/mL in net protein spin dialysis on a 9 kDa MWCO iCON spin concentrator. The Golgi apparatus fraction (for resin **R3**, Fig. 2) was collected from HCT-116 cells by use of a Golgi apparatus isolation kit (Sigma–Aldrich). The Golgi apparatus lysate was prepared from this fraction via homogenolysis by ultrasonification followed by concentration to 5 mg/mL in net protein spin dialysis on a 9 kDa MWCO iCON spin concentrator. Each fraction was either dialyzed or spin dialyzed into 50 mM MOPS, 150 mM NaCl, and 10 mM $MgCl_2$ buffer for resin coupling.

4.3. Reverse affinity resin preparation

Reverse affinity resins **R1**–**R5** (Fig. 2) were prepared by washing Affi-Gel 10 resin with an equal volume of EtOH (2×), 50% EtOH (2×), and PBS pH 7.2 at 4 °C. Immediately after washing, the subcellularly fractionated lysate containing 5 mg/mL in net protein was added, and the resin was shaken for 6 h at 4 °C. One resin was prepared for each of the five subcellular fractions (**R1**–**R5**, Fig. 2). After loading of the lysate protein, each resin was filtered and capped by treatment with an equal volume of 100 mM glycine ethyl ester in PBS at pH 7.2 containing 10 mM $MgCl_2$ for 3 h at 4 °C. The resin was harvested and washed three times with 1 mL of PBS at pH 7.2 containing 10 mM $MgCl_2$. The protein concentration on each resin was determined either by A_{280} measurement or commercial protein quantification kits (Bio-Rad). Each resin was stored at 4 °C in PBS at pH 7.2 containing 10 mM $MgCl_2$ up to 24 h prior to use.

4.4. Extract preparation

A specimen of *A. conifera* was collected at 35–40 m depth off the western shore of Monito Island near Mona Island, Puerto Rico on July 11th 2006. The sample was frozen immediately after collection and subsequently freeze-dried to afford 0.58 kg dry weight. This specimen was broken into 1–2 cm^3 pieces and soaked in a 1:1 mixture of MeOH and CH_2Cl_2 for 12 h at 4 °C. After warming to rt, the solution was filtered through a coarse sintered glass funnel and the solvent was removed by rotary evaporation. The material was then defatted by partitioning between hexanes (500 mL)

and CH_3CN (500 mL). The CH_3CN layer was collected and washed with a second aliquot of hexanes (500 mL) and then dried by rotary evaporation to afford 1.25 g of crude extract **E1** that was stored at −78 °C until used.

4.5. Reverse affinity isolation

A sample of extract **E1** (854 mg) dissolved in DMSO (5 mL) was diluted to 1 L with PBS pH 7.2. After standing for 2 h, the resulting solution was filtered through a 0.22 μm vacuum filter unit (Millipore) to remove the particulates. This solution was then added to the reservoir and air was bled from the system through a valve on the chamber. An additional 50 mL of PBS pH 7.2 was required to fill the tubing and dead space within the system. Once filled and bled of air this system was pumped between 1 cm ID polycarbonate fritted columns (Ridout Plastics) loaded with 25 mL of either resin **R1**–**R5** using a low pressure liquid diaphragm pump (KNF Neuberger) as depicted in Figure 2 and a flow rate of 0.5 mL/min at 4 °C until complete passage of the media. At this point, the system was opened, the media was removed, and the columns were washed by pumping PBS pH 7.2 (1 L) and deionized water (2 × 1 L) for 2 h each. The columns were then removed from the system and the bound materials were eluted from each column using warm 95% EtOH (200 mL). The EtOH fractions were dried by rotary evaporation.

4.6. LC/MS screening

The fractions eluted from resins **R1**–**R5** were evaluated by LC/MS analysis on an Agilent 1100 LC equipped with a 50 mm × 4.6 mm Xterra reversed-phase column with matching guard cartridge (Waters). Exemplary LC assay conditions: mobile phase A: 0.1% HCO_2H in H_2O, B: 0.1% HCO_2H in CH_3CN, gradient = 5–95% B in 30 min with post-column injection of C: 20 mM NH_4OAc in CH_3CN/H_2O (3:1), 0.2 mL/min; 2.5 μL injection volume (~10 μM sample); diode array detection was monitored at 254 nm. Data from this analysis were processed in Microsoft Excel and rendered in line format as depicted in Figure 4.

4.7. Purification

Compounds were purified by HPTLC on 5 cm × 20 cm Silica Gel RP-18 plate (EM Science) using a mixture of 3:1 CH_3CN/H_2O for elution. Samples of compounds **1**–**5** were eluted from the plates with CH_3CN and dried via rotary evaporation. The purity of each material was determined to be ⩾95% by HPLC analysis.

4.8. Degradation analyses

Degradation studies were conducted using procedures developed by Fattorusso and Mangoni.[13] The following sections provide a description of the experimental procedures and observations.

4.8.1. Methanolysis of 4

Compound **4** (100 μg) dissolved in 500 μL of 1 M HCl in 95% MeOH was incubated for 12 h at 80 °C in a sealed tube. The reaction mixture was dried under N_2 flow and the resulting material was partitioned between $CHCl_3$ (2 mL) and 20% MeOH (2 mL). Both layers were dried by N_2 flow to deliver fraction **A** (from the 20% MeOH layer) and fraction **B** (from the $CHCl_3$ layer). This process was also scaled to 1 mg of **4**.

4.8.2. Carbohydrate analysis

Fraction **A** obtained from the methanolysis of 100 μg of **4** was dissolved in anhydrous pyridine (1 mL) containing 4-dimethylamino-pyridine (10 μg) and treated with benzoylchloride (50 μL) at 0 °C. The mixture was warmed to rt and stirred for 16 h. The reaction was quenched by the addition of MeOH (0.5 mL) and dried under N_2 flow. The residue was purified by HPTLC using 5 cm × 20 cm Silica Gel 60 plate (EM Science) and eluted with a mixture of 1:1 hexanes/EtOAc to afford α-methyl-2,3,4,6-tetra-*O*-benzoyl-D-galactoside, which was identical to an authentic standard.[24] ^1H NMR (d_6-acetone) δ_H 8.13–7.33 (20H, m, Ar), 6.12 (1H, dd, J = 1.5, 3.5 Hz, H-4), 6.03 (1H, dd, J = 3.6, 10.4 Hz, H-3), 5.75 (1H, dd, J = 3.5, 10.4 Hz, H-2), 5.40 (1H, d, J = 3.6 Hz, H-1), 4.81 (1H, dd, J = 1.6, 5.6 Hz, H-5), 4.51 (1H, dd, J = 5.5, 11.1 Hz, H-6a), 4.58 (1H, dd, J = 7.0, 11.0 Hz, H-6b), 3.58 (3H, s, $-OCH_3$).

4.8.3. Sphinganine analysis

Fraction **A** obtained from the methanolysis of 1 mg of **4** was dissolved in anhydrous pyridine (2 mL) containing 4-dimethylamino-pyridine (50 μg) and treated with benzoylchloride (100 μL) at 0 °C. The mixture was warmed to rt and stirred for 16 h. The reaction was quenched by the addition of MeOH (1 mL) and dried under N_2 flow. The residue was purified by HPTLC using 5 cm × 20 cm Silica Gel 60 plate (EM Sciences) and eluting with a mixture of 1:1 hexanes/EtOAc to afford 180 μg of the perbenzoylated sphinganine fragment (see D, Fig. 8) which was characterized by high-resolution MS. HR-ESI MS: $M+Na^+$ at m/z 778.3724 (calcd for $C_{48}H_{53}NNaO_7$, 778.3720) along with a minor $M+Na^+$ at m/z 764.3559 (calcd for $C_{47}H_{51}NNaO_7$, 764.3563). Without an authentic standard, detailed NMR studies were not conducted, rather the resulting materials were examined by oxidative cleavage, as described in the following section.

4.8.4. Microscale oxidation of sphinganine fraction D

The sample of fraction **D** (180 μg) was dissolved in *t*-BuOH (300 μL) and treated by the sequential addition of 40 mM K_2CO_3 (50 μL), 25 mM $KMnO_4$ (200 μL) and 100 mM $NaIO_4$ (200 μL). The mixture was warmed to 37 °C in a sealed vial. After 18 h, the mixture was acidified with 5 M H_2SO_4 and decolorized by the addition of a saturated solution of Na_2SO_3. The mixture was diluted with 1 mL of H_2O and extracted with Et_2O (3 × 5 mL). The combined extracts were dried with Na_2SO_4. The resulting solution was treated with 2 M $TMSCHN_2$ in Et_2O (500 μL) for 1 h at rt at which point it was concentrated to ~200 μL by rotary evaporation. The resulting solution was evaluated by GC/MS. The results were as follows: methyl-heptanoate with t_R = 2.5 min with M^+ at m/z 144, methyl-6-methylheptanoate, t_R = 3.6 min with M^+ at m/z 158, methyl-octanoate, t_R = 4.4 min with M^+ at m/z 158. Relative abundances were determined by peak integration and were compared to a quantitative 1:1:1 mixture of methyl-heptanoate, methyl-6-methylheptanoate, and methyl-octanoate. These results are summarized in Figure 8.

4.8.5. Microscale oxidation of fraction B

Fraction **B** obtained from the methanolysis of 400 μg of **4** was dissolved in *t*-BuOH (150 μL) and treated by the sequential addition of 40 mM K_2CO_3 (25 μL), 25 mM $KMnO_4$ (100 μL) and 100 mM $NaIO_4$ (100 μL). The mixture was warmed to 37 °C in a sealed vial. After 18 h, the mixture was acidified with 5 M H_2SO_4 and decolorized by the addition of a saturated solution of Na_2SO_3. The mixture was diluted with 1 mL of H_2O and extracted with Et_2O (3 × 3 mL). The combined extracts were dried with Na_2SO_4. The resulting solution was treated with 2 M $TMSCHN_2$ in Et_2O (250 μL) for 1 h at rt at which point it was concentrated to ~200 μL by rotary evaporation. The resulting solution was evaluated by GC/MS. The results were as follows: methyl-heptanoate with t_R = 2.5 min and M^+ at m/z 144, methyl-6-methylheptanoate, t_R = 3.6 min, M^+ at m/z 158, methyl-octanoate, t_R = 4.4 min with M^+ at m/z 158, methyl-decanoate, t_R = 6.8 min with M^+ at m/z 186, methyl-undecanoate, t_R = 7.3 min with M^+ at m/z 200,

methyl-10-methylundecanoate, t_R = 8.1 min with M^+ at *m/z* 214 and methyl-dodecanoate with t_R = 8.9 min, M^+ at *m/z* 214. Relative abundances were determined by peak integration and were compared to a quantitative 1:1:1:1 mixture containing methyl-heptanoate, methyl-undecanoate, methyl-6-octanoate and methyl-dodecanoate. These results are summarized in Figure 8.

4.8.6. Room temperature acid hydrolysis

Compound **4** (600 μg) dissolved in 300 μL of 1 M HCl in 95% MeOH was incubated for 12 h at rt. The reaction mixture was dried under N_2 flow and the resulting material was partitioned between $CHCl_3$ (2 mL) and 20% MeOH (2 mL). The $CHCl_3$ fraction was evaluated by GC/MS indicating the presence of γ-butyrolactone, t_R = 4.5 min with M^+ at *m/z* 86.

4.8.7. Coniferoside (4)

Colorless wax, $[\alpha]_D^{25}$ −9.2 (*c* = 1.0 in MeOH); IR (NaCl plate) ν_{max} 3382, 2930, 2856, 1756, 1641, 1525, 1481, 1216, 1080 cm^{-1}; UV–vis λ_{max} (MeOH) 238 nm (ε 6900) nm; ^1H and ^{13}C NMR data are provided in Table 1. Copies of selected spectra are provided in the Supplementary data.

Acknowledgments

We thank S.-J. Nam (Scripps Institution of Oceanography) and W. Fenical (Scripps Institution of Oceanography) for confirming the isolation of compound **4** using conventional HPLC purification techniques as well as providing support in data collection and structure elucidation efforts. We also thank J. Newton (UC San Diego) and Y. Su (UC San Diego) for assistance with collection of the LC/MS and GC/MS data and J. Vicente (University of Puerto Rico), J. Marrero (University of Puerto Rico), J. C. Asencio (diver), R. Rios (diver), M. J. Lear (National University of Singapore), and the crew of the R/V Sultana for providing logistic support during the sponge collection. Financial support from a NIH-SC1 Award to ADR (Grant 1SC1GM086271-01A1) is gratefully acknowledged.

Supplementary data

Supplementary data (copies of ^1H, ^{13}C, gCOSY, TOCSY, ROESY, HSQC, and HMBC spectra of **4** in 3:1 $CDCl_3/CD_3OD$ and gCOSY and TOCSY spectra of **4** in 9:1 $CDCl_3/d_5$-pyridine) associated with this article can be found, in the online version, at doi:10.1016/j.bmc.2011.06.051.

References and notes

1. Butler, M. S. *Nat. Prod. Rep.* **2008**, *25*, 475.
2. Li, J. W.; Vederas, J. C. *Science* **2009**, *325*, 161.
3. Butler, M. S.; Newman, D. *J. Prog. Drug Res.* **2008**, *65*, 3.
4. Carlson, E. E. *ACS Chem. Biol.* **2010**, *5*, 639.
5. Hughes, C. C.; Fenical, W. *Chemistry* **2010**, *16*, 12512.
6. Thomas, T. R.; Kavlekar, D. P.; LokaBharathi, P. A. *Mar. Drugs* **2010**, *8*, 1417.
7. Newman, D. J.; Cragg, G. M. *Curr. Opin. Invest. Drugs* **2009**, *10*, 1280.
8. La Clair, J. J. *Nat. Prod. Rep.* **2010**, *27*, 969.
9. Bugni, T. S.; Richards, B.; Bhoite, L.; Cimbora, D.; Harper, M. K.; Ireland, C. M. *J. Nat. Prod.* **2008**, *71*, 1095.
10. Koehn, F. E. *Prog. Drug Res.* **2008**, *65*, 177.
11. Koehn, F. E.; Carter, G. T. *Nat. Rev. Drug Disc.* **2005**, *4*, 206.
12. Rodríguez, A. D.; Lear, M. J.; La Clair, J. J. *J. Am. Chem. Soc.* **2008**, *130*, 7256.
13. Costantino, V.; Fattorusso, E.; Imperatore, C.; Mangoni, A.; Freigang, S.; Teyton, L. *Bioorg. Med. Chem.* **2008**, *16*, 2077.
14. Costantino, V.; Fattorusso, E.; Imperatore, C.; Mangoni, A. *J. Org. Chem.* **2004**, *69*, 1174.
15. Costantino, V.; D'Esposito, M.; Fattorusso, E.; Mangoni, A.; Basilico, N.; Parapini, S.; Taramelli, D. *J. Med. Chem.* **2005**, *48*, 7411.
16. Andreyev, A. Y.; Fahy, E.; Guan, Z.; Kelly, S.; Li, X.; McDonald, J. G.; Milne, S.; Myers, D.; Park, H.; Ryan, A.; Thompson, B. M.; Wang, E.; Zhao, Y.; Brown, H. A.; Merrill, A. H.; Raetz, C. R.; Russell, D. W.; Subramaniam, S.; Dennis, E. A. *J. Lipid Res.* **2010**, *51*, 2785.
17. Riboni, L.; Giussani, P.; Viani, P. *Adv. Exp. Med. Biol.* **2010**, *688*, 24.
18. Mosmann, T. *J. Immunol. Methods* **1983**, *65*, 55.
19. Veerapen, N.; Reddington, F.; Bricard, G.; Porcelli, S. A.; Besra, G. S. *Bioorg. Med. Chem. Lett.* **2010**, *20*, 3223.
20. Oskouian, B.; Saba, J. D. *Adv. Exp. Med. Biol.* **2010**, *688*, 185.
21. Ekiz, H. A.; Baran, Y. *Int. J. Cancer* **2010**, *127*, 1497.
22. Szilágyi, Z.; Pócsfalvi, G.; Costantino, V.; Mangoni, A.; Malorni, A.; Fattorusso, E. *Rapid Commun. Mass Spectrom.* **2004**, *18*, 2989.
23. Trainer, M. A.; Charles, T. C. *Appl. Microbiol. Biotechnol.* **2006**, *71*, 377.
24. Esmurziev, A.; Simić, N.; Sundby, E.; Hoff, B. H. *Magn. Reson. Chem.* **2009**, *47*, 449.